Available online at www.sciencedirect.com
ScienceDirect
Journal of Pharmaceutical and Biomedical Analysis 47 (2008) 303–311
JOURNAL OF PHARMACEUTICAL AND BIOMEDICAL ANALYSIS
www.elsevier.com/locate/jpba

The chemistry of multi-protic drugs Part 1: A potentiometric, multi-wavelength UV and NMR pH titrimetric study of the micro-speciation of SKI-606

Karl J. Box [a], Rachel E. Donkor [b], Philip. A. Jupp [b], Ian P. Leader [b], David F. Trew [b,*], Christopher H. Turner [c]

[a] *Sirius Analytical Instruments Ltd., Riverside, Forest Row Business Park, Forest Row, East Sussex RH18 5DW, UK*
[b] *Analytical Research and Development, Wyeth Research (UK), Barwell Lane, Gosport, Hampshire PO13 0AU, UK*
[c] *NMR Consultant, The Shambles, 1 Firestone Glade, Wootton Bridge, Ryde, Isle of Wight PO33 4LH, UK*

Received 29 October 2007; received in revised form 10 December 2007; accepted 8 January 2008
Available online 18 January 2008

Abstract

The application of a combination of potentiometric, spectrophotometric and nuclear magnetic resonance (NMR) pH titrimetric methodology to measure the macroscopic and to calculate the microscopic protonation constants of SKI-606, a multi-protic compound is described. This compound is currently under evaluation as a candidate drug for the treatment of cancer. SKI-606 was found to have four protonatable sites in the pH range 1–12. Two of these were well separated ($\Delta \log K > 3$), whereas the other two overlapped to form a di-protic system. Protonation at only two of the sites yielded a change in the UV spectrum, but the protonation at all four sites could be monitored by NMR. The microscopic equilibrium constants were calculated from the NMR data, which were used in combination with the potentiometric macroscopic constants to calculate the distribution of micro-species.

Keywords: Potentiometric; Spectrophotometric and nuclear magnetic resonance pH titration; Macroscopic and microscopic equilibrium constants

1. Introduction

It has long been recognized that the acid–base chemistry of a drug substance plays a pivotal role in the development of a new drug. The acid–base chemistry will determine whether the drug is in ionic or non-ionic form, which in turn will affect its solubility and rate of dissolution in the gastrointestinal tract, permeability across biological membranes [1], bioavailability and access to the site of action. The pharmacokinetics and pharmacodynamics of a drug are often determined by its acid–base chemistry, which can also be used to predict the extent of receptor binding and hypothesize the mode of action [2]. Indeed it has been proposed that the bioavailability of drugs is determined by the predominant protonation state at biological pH [3].

Equilibrium constants (expressed either as dissociation constants pK_a or protonation constants $\log K$) are normally used to characterize, in numerical terms, the acid–base chemistry of a compound that has either a single protonatable site or multiple sites with well-separated (>3 pH units) equilibrium constants [4], and are often referred to as the macroscopic equilibrium constants [5]. However, in a molecule with overlapping $\log K$s, these constants characterize the acid–base equilibrium as a whole but fail to provide information on specific protonatable sites. A compound with n protonatable sites can potentially exist in 2^n protonation states, called micro-species. The equilibrium constants between the different micro-species are referred to as the microscopic equilibrium constants [5].

Potentiometric pH titration is the usual method for the determination of equilibrium constants in aqueous solution for readily soluble compounds [2]. With care, good reproducible results ($\log K \pm 0.03$) can be obtained by this method for acids and bases having $\log K$ values between 2.5 and 10.5. Outside this

* Corresponding author. Tel.: +44 1329 507747; fax: +44 1329 507800.
E-mail address: trewd@wyeth.com (D.F. Trew).

0731-7085/$ – see front matter © 2008 Elsevier B.V. All rights reserved.
doi:10.1016/j.jpba.2008.01.015

range potentiometric pH titration suffers from the limitation of interference due to the titration of the water solvent, as more analyte is required to overcome the buffering effect of titrating the water [6]. This can result in erroneous log *K* determination, particularly if low concentrations have to be used due to poor solubility. The problem of low aqueous solubility may be overcome by the addition of an organic co-solvent [7]. The lower dielectric constant of a water/co-solvent mixture usually suppresses ionization resulting in higher log *K* values for acids and lower values for bases. As the log *K* values obtained relate to the particular solvent used, extrapolation procedures such as the Yasuda–Shedlovsky method must be employed to calculate log *K* values at zero co-solvent [7]. Also it is important to note that potentiometric pH titration cannot provide site-specific information.

UV spectrophotometric pH titration has been used as an alternative method to measure the log *K* values of compounds having high absorption coefficients at concentrations as low as 1 μM [8]. In this study, multi-wavelength spectrophotometric techniques, in conjunction with target factor and principal component analysis procedures, and employing dip-probe technology [8,9] have been used. Spectrophotometric titration requires the compound under investigation to possess a chromophore(s) in close proximity to the site(s) of protonation in order for the protonated and unprotonated species to exhibit sufficient spectral differences. Spectrophotometric methods cannot always identify the site of protonation especially in complex molecules.

Nuclear magnetic resonance (NMR), with its ability to directly observe the magnetic environment of a particular nucleus can readily monitor the extent of protonation of an acidic or basic site and does not suffer from the above limitations [5]. NMR pH titration is able to observe each of the nuclei in a compound and thus identify the exact site of protonation. NMR has the limitation that it is relatively insensitive, when compared with spectrophotometric techniques and is a relatively time consuming technique which is not readily automated.

Each of the three analytical techniques discussed above have advantages and disadvantages and each yields different information, but a combination of all three techniques is often useful in the profiling of complex molecules. Although this strategy is not unprecedented it is seldom used in practice.

Wyeth has a research program on 4-anilino-3-quinolinecarbonitrile compounds as kinase inhibitors [10] and this has led to the identification of a number of compounds as potential drug candidates for the treatment of a variety of diseases [11]. This paper describes the application of a combination of potentiometric, spectrophotometric and NMR titration techniques to the microscopic profiling of one of these compounds SKI-606 (Fig. 1). Also in this paper we describe some unusual experimental procedures to allow for the NMR measurements to be carried out in non-deuterated solvents and to speed up the collection of NMR data.

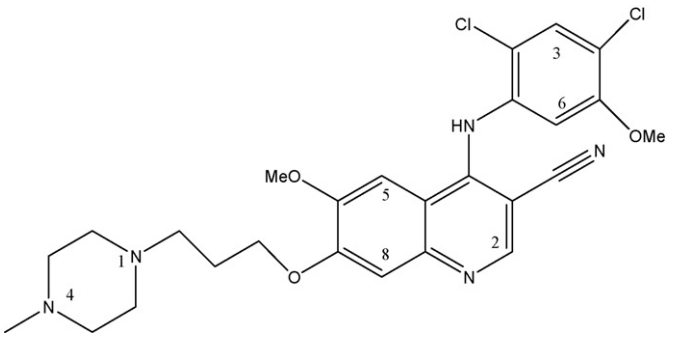

Fig. 1. Structure of SKI-606.

2. Experimental

2.1. Materials

SKI-606 is a Wyeth development compound and was obtained from the Chemical Development Department, Rouses Point NY. The sample had an anhydrous purity of 99.8% and was used without further purification. Potassium chloride, potassium dihydrogen phosphate, hydrochloric acid, potassium hydroxide, sodium hydroxide (all AR grade) and methanol (HPLC grade) were obtained from Fisher Scientific (Loughborough, UK). Where appropriate, solutions were prepared in deionized water of resistivity $>10^{14}$ Ω cm. Deuterated benzene (NMR grade) was obtained from Aldrich (Dorset, UK).

2.2. Potentiometric and spectrophotometric methodology

Potentiometric titrations were performed with a Sirius GLpKa^{TM} titrator (Sirius, Forest Row, East Sussex, UK) fitted with a combination Ag–AgCl pH electrode. Titrations were carried out from pH2 to pH12 in 0–68% (w/w) methanol:water mixtures using standardized 0.5 M HCl and 0.5 M KOH. Solutions were kept at constant temperature ($t = 25 \pm 1$ °C) and under an argon atmosphere. The ionic strength ($I = 0.17$ M KCl) was calculated on a point-by-point basis during the whole titration and pK_as are reported at (or corrected to) the average ionic strength of the solution. The ionic strength did not change by more that 3 mM during the titrations. A temperature probe monitored the temperature during the course of the titration. Precision dispensers were connected to narrow polyimide-clad quartz capillary (500 μm inside diameter) tubes and were capable of delivering small reproducible aliquots of known volume. An overhead stirrer was connected to a motor whose speed of rotation was controlled by the instrument. The instrument was controlled and results were calculated using Sirius RefinementPro^{TM} (v2.2.2.8) software. Multi-wavelength UV spectrophotometric titrations were performed with the Sirius D-PAS^{TM} ultra-violet spectrometer (Sirius, Forest Row, East Sussex, UK) attachment for the GLpKa. The D-PAS was fitted with a bifurcated fibre-optic probe with path length of 1 cm (Hellma, UK). Spectrophotometry can be applied for log *K* measurement provided that the compound has a chromophore in proximity to the ionization centre, and the absorbance changes sufficiently as a function of pH. Evidence for sample precipitation can be found (in both potentiometric and multi-wavelength UV pK_a titrations) by using the fibre-optic dip-probe to detect light scattering at 600 nm. The general procedures, calculations

and instrumentation have been described in previous publications [7–9,12–14]. Potentiometric titrations were carried out at SKI-606 sample concentrations that varied from 0.28 mM (at 0% methanol) to 1.15 mM (at 68% methanol) whilst UV spectrophotometric titrations were at sample concentrations of 19.5–42.4 μM. Estimated uncertainties in the log *K* measurements were between ±0.04 and ±0.12 for the potentiometric study, and between ±0.05 and ±0.1 for the spectrophotometric study.

2.3. Nuclear magnetic resonance methodology

NMR pH titrations were carried out in 25.5–68% (w/w) methanol:water mixtures at sample concentrations of 2–3 mM. Attempts to obtain NMR data in solvents containing lower proportions of methanol were unsuccessful due to precipitation of the SKI-606. In order to avoid inaccuracies inherent in converting equilibrium constants measured in deuterated solvents, to equilibrium constants in protonated solvents, NMR titrations were carried out in non-deuterated solvents. The pH of the solutions was measured with an InLab 415 pH glass electrode (Mettler Toledo, Urdorf, Switzerland) and an IQ150 pH Meter (IQ Scientific Instruments, Inc., Carlsbad, US). The electrode was calibrated in each solvent mixture following the procedure described by Mazák et al. [15]. In a typical experiment a solution of 2–3 mM SKI-606 (20 ml) in the appropriate solvent mixture was first acidified to ca. pH 1 with HCl, in the appropriate solvent mixture, and then titrated by adding aliquots (10 μl) (*via* a Hamilton syringe) of solutions of 10, 1.0 and 0.1 M NaOH, in the appropriate solvent mixture. These experiments were carried out at a similar ionic strength to that used in the potentiometric and spectrophotometric studies; it is estimated that the ionic strength change during these titrations was less than 3 mM. At selected pH values, a 500 μl aliquot of the solution was removed and placed in a 5 mm NMR tube. A coaxial insert tube (Z27,851-3 Aldrich, Dorset, UK) containing benzene d_6 was inserted into the NMR tube, this was used to obtain a deuterium lock and the benzene signal at 7.150 ppm (due to residual benzene) was used as an external reference to measure the chemical shifts. Any bulk shifts between the two independent solutions were monitored by checking the shifts of signals due to non-titratable groups.

^{1}H NMR spectra were obtained using a JEOL GSX-270 FT NMR spectrometer operating at 270 MHz and controlled by the Delta Eclipse software package. As the study only required the measurement of the chemical shift of protons close to titratable groups and did not require integration information, the standard ^{1}H NMR experiment was modified as follows: data points reduced from 16 to 4 K, pulse angle increased from 45 to full 90°, delay (relaxation) time reduced from 2 to 0.1 s, exponential multiplier for processing increased from 0 to 0.5 Hz. Under these experimental conditions, spectra with a signal to noise ratio of ca. 10:1 for the quinoline-*2H* singlet could be recorded in 40 scans (<2 min), with a spectral resolution of 0.0024 ppm/data point. This modified NMR experiment does not yield accurate integration but this information is not required in the present study. An added advantage of this modified experiment is that the signals due to the solvents are much reduced while retaining most of the area of the sample signals. Assignment of the signals was achieved using standard ^{1}H, ^{13}C, Distortionless Enhancement by Polarization Transfer (DEPT), homo and hetero nuclear Correlation Spectroscopy (COSY), Nuclear Overhauser Effect Spectroscopy (NOESY) and Correlation by Long Range Coupling (COLOC) NMR experiments.

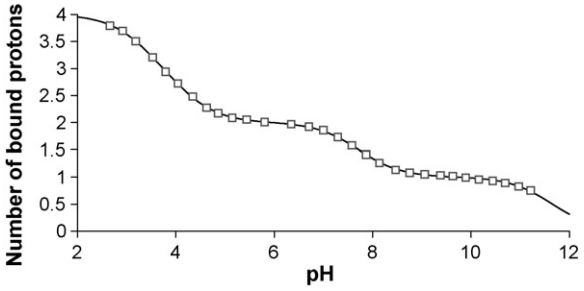

Fig. 2. Typical Bjerrum plot of SKI-606.

The extent of protonation (E_p) (mole fraction) at a specific site was calculated from NMR chemical shift data using Eq. (1)

$$E_p = \frac{\delta_{pH} - \delta_B}{\delta_{BH} - \delta_B} \quad (1)$$

where δ_{BH}, δ_B and δ_{pH} are the chemical shifts of the fully protonated species, fully deprotonated and at the measured pH, respectively.

3. Results

3.1. Potentiometric titrations

Potentiometric titration curves were converted into Bjerrum plots [16] which show the number of bound protons *per* molecule as a function of pH. Protonation constants (log *K*) are found at the half proton intercepts (Fig. 2). These revealed the presence of four protonatable sites over the pH range 1–12 and the protonation constants are presented in Table 1. In particular it can be seen from Fig. 2 that the inflections over the pH of 11–12 and 6.5–8.5 each correspond to one bound proton, whereas the inflection over the pH range 2–5 corresponds to two bound protons, thus demonstrating the presence of two overlapping log *K*s. Yasuda–Shedlovsky ($\log K + \log [H_2O]$ versus $1000/\varepsilon$) plots (where ε = dielectric constant) were constructed from the measured protonation constants and the slopes (*a*), intercepts (*b*) and regression coefficients (*r*) are reported in Table 1. In order to assess the accuracy of the Yasuda–Shedlovsky extrapolation procedure the extrapolated aqueous log *K* values for three of the four equilibrium constants are also shown. Expressing the differences between the extrapolated and measured log *K* values as $\Delta \log K = \log K_{extrapolated} - \log K_{measured}$, the following values were obtained: $\Delta \log K_2 = 0.12$, $\Delta \log K_3 = 0.05$, $\Delta \log K_4 = -0.01$. The results for the first protonation constant K_1 (highest log *K* value) should be viewed with caution. In solutions above pH 9 with methanol composition less than 22% the sample precipitated and the log K_1 values are estimates. In addition, the sample concentration was too low for accurate determination of log K_1 due to interference from the titration

Table 1
Potentiometric protonation constants for SKI-606 in different proportions of methanol:water

% w/w methanol:water	log K_1	log K_2	log K_3	log K_4
0	11.20[a]	7.92[b]	4.75	3.78
0	11.20[a]	7.93[b]	4.75	3.80
6.9	11.25[a]	7.89[b]	4.87	3.69
11.8	11.30[a]	7.92[b]	4.74	3.66
17.5	11.35[a]	7.83[b]	4.64	3.67
22.2	11.38	7.91	4.53	3.55
30.0	11.58	7.85	4.36	3.45
39.1	11.66	7.72	4.18	3.31
46.7	11.46	7.66	4.07	3.21
56.0	11.55	7.51	3.90	3.14
67.9	11.33	7.26	3.70	2.81
Yasuda–Shedlovsky parameters ($\log K + \log [H_2O] = b + a/\varepsilon$)				
a	−16.8	−163.7	−232.3	−196.7
b	13.21	11.85	9.48	8.00
r	−0.867[c]	−0.992	−0.990	−0.997
Extrapolated aqueous log K	11.20	8.04	4.80	3.77

[a] These values are estimates due to sample precipitation.
[b] Precipitation occurred above this pK_a.
[c] Correlation for K_1 is calculated on the values from 22.2 to 67.9% methanol.

of water [6]. This protonation constant was readily measured using the spectrophotometric technique.

3.2. UV spectrophotometric titrations

The spectrophotometric pH study showed that of the four protonatable groups detected during the potentiometric study only two of these yielded a change in the UV spectrum. The protonation constants measured in the spectrophotometric study are presented in Table 2, and correspond to the first and third constants determined in the potentiometric study, respectively. As with the potentiometric study Yasuda–Shedlovsky plots were constructed from the measured protonation constants and the slopes (a), intercepts (b) and regression coefficients (r) are also reported in Table 2. Again in order to assess the accuracy of the Yasuda–Shedlovsky extrapolation procedure the two calculated aqueous log K values are also shown. The correlation coefficient for the highest equilibrium constant is rather low at −0.531. Yet the differences between the extrapolated and measured log K values (expressed as defined above) of between −0.08 and 0.10 for $\Delta \log K_{uv1}$ and between −0.12 and 0.13 for $\Delta \log K_{uv2}$, demonstrates the overall consistency of the spectrophotometric data. The absorbance profile as a function of wavelength and pH is shown in Fig. 3. The profile was independent of the solvent composition and as one of the sites that have an overlapping log K did not yield any change in the UV spectrum, this prevented accurate calculation of the micro-constants using the spectrophotometric data [17].

Table 2
Spectrophotometric protonation constants for SKI-606 in different proportions of methanol:water

% w/w methanol:water	log K_{uv1}	log K_{uv2}
0	11.26	4.83
0	11.22	4.86
0	11.20	4.89
5.2	11.26	4.80
10.0	11.32	4.69
11.2	11.34	4.68
17.5	11.38	4.56
25.0	11.49	4.37
26.4	11.41	4.43
34.5	11.49	4.29
36.6	11.53	4.19
45.3	11.55	4.08
45.4	11.52	4.13
48.7	11.62	4.01
55.7	11.58	3.97
58.1	11.67	3.91
68.3	11.64	3.86
Yasuda-Shedlovsky parameters ($\log K + \log [H_2O] = b + a/\varepsilon$)		
a	−12.07	−211.6
b	13.18	9.198
r	−0.531	−0.983
Extrapolated aqueous log K	11.28	4.77

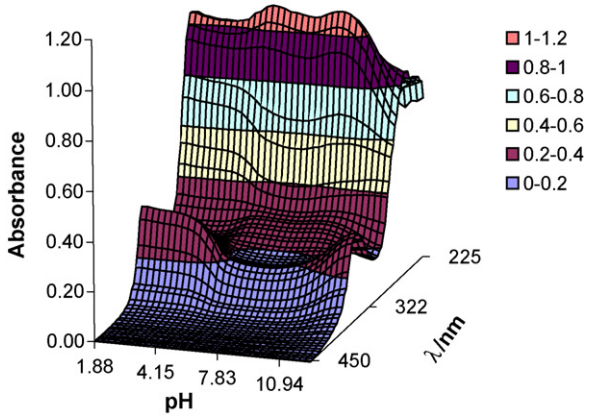

Fig. 3. UV absorption spectra of SKI-606 in water.

3.3. Nuclear magnetic resonance titrations

The NMR study showed the position of the four protonatable sites. Fig. 4 is an example of a typical ^{1}H NMR

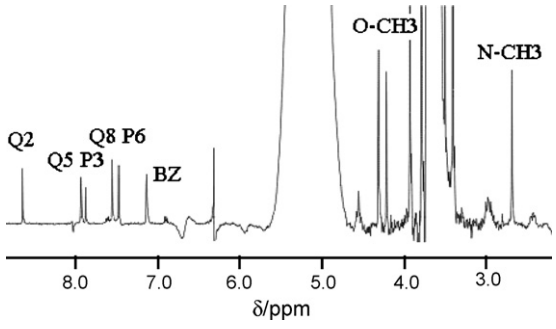

Fig. 4. Typical NMR spectrum of SKI-606. Q2, Q5 and Q8 = quinoline 2H, 5H and 8H, P3 and P6 = 2,4-dichloro-5-methoxyphenyl 3H and 6H, N–CH_3 = piperizine N–CH_3, O–CH_3 = methoxy CH_3, respectively. BZ = benzene external reference signal.

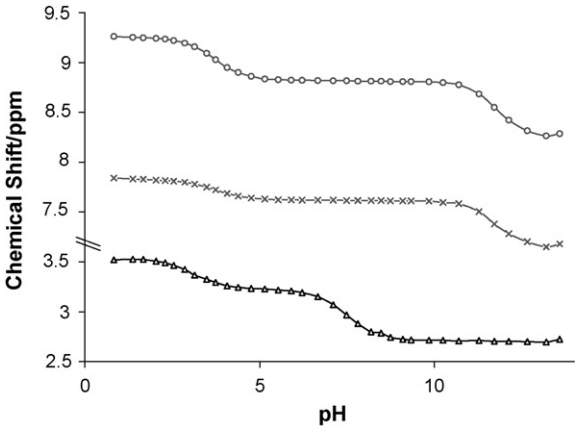

Fig. 5. Typical NMR titration curves in water: methanol solvent. (◯) Quinoline *2H*, (x) 2,4-dichloro-5-methoxyphenyl *6H*, (Δ) piperizine N–CH_3.

spectrum of SKI-606 in methanol:water. Although the water and methanol do give very large peaks ($\delta = 5.1$ and 3.6 ppm, respectively) these do not interfere with the key signals. In the current study, the signals for the quinoline *2H* ($\delta = 8.67$ ppm), 2,4-dichloro-5-methoxyphenyl *6H* ($\delta = 7.491$ ppm) and piperizine N–CH_3 ($\delta = 2.685$ ppm), protons proved to be excellent probes for monitoring the protonation of the different sites and the quinoline *2H* signal could be used to accurately determine the extent of protonation of the 1-quinoline site. Chemical shifts for the remaining protons were as follows: quinoline *5H* ($\delta = 7.952$ ppm), quinoline *8H* ($\delta = 7.571$ ppm), 2,4-dichloro-5-methoxyphenyl *3H* ($\delta = 7.897$ ppm), and the two methoxy CH_3 ($\delta = 4.315$ and 3.930 ppm). The propyl and piperizine ring signals are in the region of 2.3–3.5 ppm, some of which are overlapped or obscured. The benzene reference signal (due to residual non-deuterated benzene in the deuterium lock solvent) is seen at 7.150 ppm.

Typical NMR titration curves for these signals are shown in Fig. 5. The titration curves for both the quinoline *2H* and 2,4-dichloro-5-methoxyphenyl *6H* protons show inflections in the regions of pH 3–5 and 11–13. The titration curve for the piperizine N–CH_3 signal also shows two inflections but in the regions of pH 2–4 and 6–8. The relative magnitudes of the inflections for all three signals in the different pH regions are different and these are summarized in Table 3. The significance of these observations will be discussed below.

Table 3
Magnitude of chemical shift change ($\Delta\delta$/ppm) for the quinoline 2H (Q2), 2,4-dichloro-5-methoxyphenyl *6H* (P6), and piperizine N–CH_3 (N–CH_3) signal over different pH ranges

pH Range	Q2	P6	N–CH_3
2–4	No inflection	No inflection	0.33
3–5	0.45	0.2	No inflection
6–8	No inflection	No inflection	0.48
11–13	0.56	0.45	No inflection

3.4. Evaluation of micro-constants

The calculation of the four microscopic equilibrium constants of a diprotic system requires at least three independent pieces of information. Two of these are the macroscopic equilibrium constants (measured during the potentiometric study), while the third must come from data that relates exclusively to a single site [5]. In the current study, this information came from the NMR titration curve for the quinoline *2H* proton. In the pH 3–5 region this curve is influenced by protonation at a single site, in particular this curve shows no inflection in the pH 6–8 region demonstrating that it is not influenced by protonation on the piperizine ring. NMR titration methodology yields extent of protonation (E_p) data at a specific site as a function of pH *via* Eq. (1). This is the ratio of the total concentration of the protonated species to the total concentration of all species present at the particular pH. Thus, the extent of protonation of the quinoline nitrogen, in terms of concentration of micro-species, is given by Eq. (2) (see Fig. 6 for numbering of species). The first micro-constant (k_1) was calculated using Eq. (3) and the remaining micro-constants were calculated using Eqs. (4) and (5) [5]. (Note: species **1** and **2** are below 1% in the pH region 1–6 and are, therefore, not included).

$$E_p = \frac{[\mathbf{4}] + [\mathbf{6}]}{[\mathbf{3}] + [\mathbf{4}] + [\mathbf{5}] + [\mathbf{6}]} \quad (2)$$

$$k_1 = \frac{(1 + K_3[H^+] + K_3K_4[H^+]^2)E_p - K_3K_4[H^+]^2}{[H^+]} \quad (3)$$

$$K_3 = k_1 + k_2 \quad (4)$$

$$K_3K_4 = k_1k_3 = k_2k_4 \quad (5)$$

Table 4 contains the macroscopic ($\log K$) and microscopic ($\log k$) protonation constants of SKI-606 in different mixtures of methanol:water. Because of the problems experienced dur-

Table 4
Macroscopic and microscopic protonation constants for SKI-606 in selected solvent mixtures

% w/w methanol:water	Macroscopic protonation constants				Microscopic protonation constants			
	$\log K_1$	$\log K_2$	$\log K_3$	$\log K_4$	$\log k_1$	$\log k_2$	$\log k_3$	$\log k_4$
0	11.2	7.93	4.75	3.79	4.34[a]	4.54	4.20	4.00
25	11.3[a]	7.86[a]	4.48[a]	3.52[a]	4.39	3.75	3.61	4.25
40	11.7	7.72	4.18	3.31	3.92	3.83	3.57	3.66
47	11.6[a]	7.66	4.07	3.21	3.74	3.80	3.54	3.48
68	11.6	7.26	3.7	2.81	3.67	2.52	2.84	3.99

[a] Calculated by extrapolation using the Yasuda–Shedlovsky procedure.

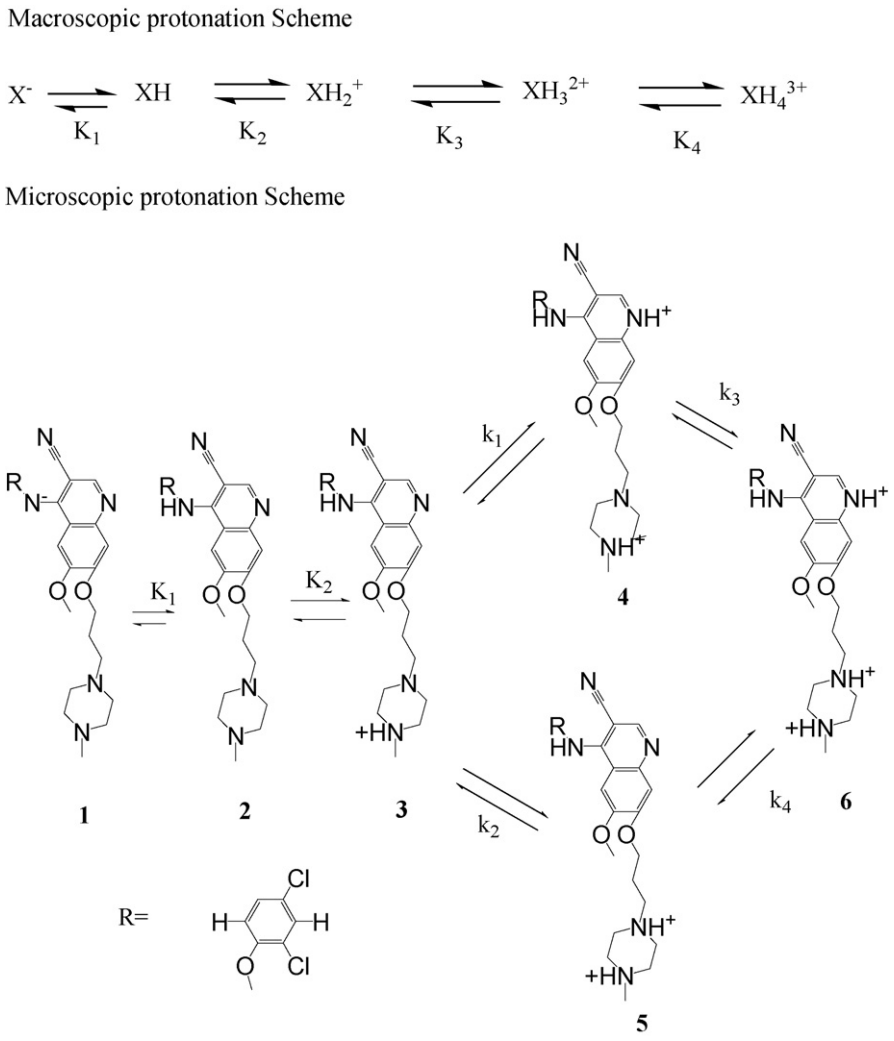

Fig. 6. Protonation scheme for SKI-606.

ing the potentiometric study with the determination of $\log K_1$ these results come from the spectrophotometric study. The values for $\log K_2$ through $\log K_4$ come from the potentiometric study. The calculated values for $\log k_1$ were converted into a Yasuda–Shedlovsky plot which allowed for the estimation of $\log k_1$ in water. The Yasuda–Shedlovsky parameters were as follows: $a = -175.4$, $b = 8.350$, $r = -0.920$.

4. Discussion

4.1. Identification of the site of protonation

A valuable quality of NMR methodology is the ability to directly observe each nucleus in a compound, and this allows for the unambiguous assignment of each protonatable site to a specific equilibrium constant. The potentiometric study showed that SKI-606 has four sites that are protonated over the pH range 1–12. The spectrophotometric study showed that only two of these influenced the UV spectrum of the molecule. The potentiometric and spectrophotometric studies showed that the $\log K$ solvent composition profile of K_1 increased with increasing methanol content. As increasing the organic content of the solvent usually suppresses ionization, this is usually indicative of an acidic centre. Conversely the decrease in $\log K$ with an increase in the organic content of the solvent seen with K_2, K_3 and K_4 is indicative of basic centres. The spectrophotometric study also showed that K_1 was UV active. This suggests that the first equilibrium constant (K_1) relates to the secondary amine bridging the quinoline and 2,4-dichloro-5-methoxyphenyl moieties. This is supported by the UV spectra in Fig. 3. As the pH is increased from pH 9 to 12 there is a large increase in absorbance in the 300–400 nm region ($\lambda_{max} = 350$ nm), indicative of an increase in conjugation as the pH is raised. Further evidence in support of this assignment comes from the magnitude of the inflections in the NMR titration curves (Table 3). The magnitude of the change in chemical shift is greatest for nuclei close to the site of protonation and rapidly diminishes with increasing distance [16]. In Fig. 5, the magnitude of the inflections of the curves for the quinoline *2H* and the 2,4-dichloro-5-methoxyphenyl *6H* protons in the pH 11–13 region are quite similar at ca. 0.56 and 0.45 ppm, respectively, and this suggests the site of protonation is situated on the nitrogen bridge between these two groups.

Table 5
Mole percentages of micro-species of SKI-606 at selected pH in different solvent mixtures

	0 % (w/w) methanol:water				25 % (w/w) methanol:water				68 % (w/w) methanol:water			
pH	2.0	5.0	6.8	7.5	2.0	5.0	6.8	7.5	2.0	5.0	6.8	7.5
Micro-species[a]												
2	0	0	7	27	0	0	8	30	0	0	26	63
3	0	63	93	73	0	76	92	70	0	96	74	37
4	1	14	0	0	2	19	0	0	13	4	0	0
5	1	22	0	0	1	4	0	0	1	0	0	0
6	98	2	0	0	97	1	0	0	86	0	0	0

[a] See Fig. 6 for micro-species numbering.

The second macroscopic protonation constant (K_2) measured in the potentiometric study showed no equivalent constant in the spectrophotometric study. This means that the site of protonation is remote from the chromophore, and this was confirmed in the NMR study where the titration curve for the quinoline *2H* and the 2,4-dichloro-5-methoxyphenyl *6H* protons showed no inflections in the pH 6–8 region. The titration curve for the piperizine N–C*H*$_3$ protons showed two inflections, one in the pH 6–8 region and the second in the pH 3–5 region. The magnitude of the inflection in the pH 6–8 region is 0.48 ppm whereas in the pH 3–5 region the magnitude is 0.33 ppm. Thus, this protonation constant (K_2) can be assigned to protonation at the 4-piperizine nitrogen.

In contrast to the first two macroscopic protonation constants, the third and forth macroscopic protonation constants differ by less than three pH units and thus, cannot be assigned to individual protonation sites, but instead only describe the overall stoichiometry of the profile [18]. The site-specific protonation is described below.

4.2. Protonation scheme and distribution of micro-species

The macroscopic and microscopic protonation schemes for SKI-606 are shown in Fig. 6. The potentiometric and spectrophotometric studies showed that SKI-606 has a total of four protonatable sites as shown in the macroscopic protonation scheme. These studies also showed that two of the protonation constants (K_1 and K_2) were well separated ($\Delta \log K_a > 3$), whereas the remaining two overlap to form a diprotic system. The detailed sub-molecular protonation scheme for SKI-606 is shown in the microscopic protonation scheme of Fig. 6. X^-, XH, XH_2^+ and XH_4^{3+} in the macroscopic scheme correspond to species **1**, **2**, **3** and **6** in the microscopic scheme, respectively, whereas XH_3^{2+} is equivalent to the sum of species **4** and **5**. Species **1**, which is the predominant micro-species above pH 11, is the fully deprotonated species and consists of an anionic amide nitrogen atom bridging the quinoline and 2,4-dichloro-5-methoxyphenyl moieties. Deprotonation of an amine normally requires strongly basic conditions. In this case the relatively low protonation constant is attributed to the number of strongly electron withdrawing groups in the vicinity of this acidic centre. Protonation of **1** yields the SKI-606 free base (species **2**) this is then protonated at the 4-piperizine nitrogen to yield the mono-cation, (species **3**). Species **2** and **3** are the predominant micro-species between pH 8 and 11, and pH 5 and 8, respectively. It is noted that although the second step in the protonation of SKI-606 takes place predominantly at the 4-piperizine nitrogen there is also a small contribution (estimated at <2%) at the 1-piperizine site that has not been quantified in this study. Up to this point protonation proceeds essentially in a sequential manner, however, as the last two macroscopic protonation constants (K_3 and K_4) differ by less than three log units, protonation can occur at either the quinoline nitrogen atom to form species **4** or at the 1-piperizine nitrogen atom to form **5**. Species **4** and **5** have the same chemical composition but differ in the site of protonation; they are, therefore, proton isomers.

The macroscopic and microscopic protonation constants enable the calculation of the distribution of micro-species and this is shown in Fig. 7 for SKI-606 in water. This shows that species **1**, **2** and **3** are the predominant species above pH 11.2, between 11.2 and 8.0 and between 8.0 and 4.8, respectively, and shows that protonation is occurring in a stepwise manner. Between pH 4.8 and 3.8 the two isomeric di-cationic species **4** and **5** are the predominant species, whereas below pH 3.8 the tri-cationic species **6** predominates. The mole percent of the different micro-species in different solvent compositions at four biologically relevant pH values (2.0, 5.0, 6.8 and 7.5), representing conditions in the stomach, small intestine under fed

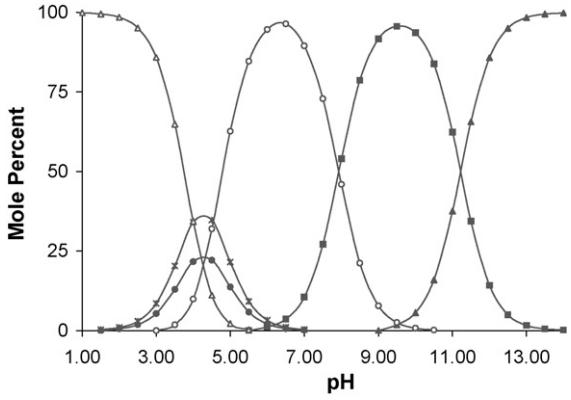

Fig. 7. Distribution of SKI-606 micro-species in water as a function of pH. (▲) Species **1**, (■) species **2**, (◯) species **3**, (●) species **4**, (x) species **5**, (△) species **6**.

Table 6
Comparison of the macroscopic equilibrium constants with predicted values using popular prediction programs

	$\log K_1$	$\log K_2$	$\log K_3$	$\log K_4$
Experimental	11.2	7.92	4.75	3.79
Program	NH	4-piperizine	quinoline	1-piperizine
Compudrug	Not predicted	8.2	4.4	3.0
ACDLabs	Not predicted	7.8	5.2	3.7
Pharma Algorithms	Not predicted	4.3	3.5	8.1
Marvin	Not predicted	8.4	4.4	2.6

and fasted conditions and blood [15,19], are listed in Table 5. Under gastric conditions the tri-cationic species **6** is the predominant species under all solvent conditions and species **4** and **5** are present in small amounts. This makes SKI-606 very soluble under gastric conditions resulting in rapid dissolution of this drug in the stomach. Under intestinal conditions the mono-cationic species **3** is the predominant micro-species present with the di-cationic species **4**, **5** and tri-cationic **6** also present under both fed and fasted conditions. The absorption of drugs across the intestinal membrane most readily occurs when the drug is in an uncharged state [1]. As SKI-606 is predominantly in the form of cationic species in the small intestine, this may limit the permeability of this compound. Furthermore, there are some differences in the species present under fed and fasted conditions which may lead to differences in absorption under these conditions. At pH 7.5 SKI-606 exists in two forms, namely the SKI-606 free base **2** and the mono-cation **3**. In a recent 'docking' analysis [20] it was calculated that SKI-606 interacts with the active form of the Src kinase *via* the quinoline and 2,4-dichloro-5-methoxyphenyl moieties and the 4-methylpiperizine is orientated away from the receptor. Thus, the protonation state of the 4-methylpiperizine nitrogen would not be expected to influence the *in vivo* mode of action of SKI-606.

4.3. Comparison of experimental macroscopic equilibrium constants with computer predictions

It is a common practice in the pharmaceutical industry to employ software to predict the $\log K$s of compounds under investigation. These are generally based on linear free energy relationships such as the Hammett and Taft equation. A comparison of the predicted macroscopic constants using four popular computer prediction programs with the experimentally measured values in water is presented in Table 6. Significantly none of the programs predicted the first protonation ($\log K_1$). The first protonation constant predicted by all of the programs agrees fairly well with the second experimental macroscopic constant $\log K_2$, although the Pharma Algorithms program has incorrectly assigned the site of protonation as the 1-piperizine site instead of the 4-piperizine site. However, only one of the second and third predicted macro-constants (corresponding to experimental $\log K_3$ and $\log K_4$) agrees with the experimentally determined values. This demonstrates that predicted equilibrium constants should be interpreted with caution.

5. Conclusions

In this paper, we have described how a combination of potentiometric, spectrophotometric and NMR pH titrimetric methodology can be employed to profile the acid–base properties of a complex multi-protic drug with four protonatable sites. Potentiometric titrations were able to readily measure three of the four macroscopic protonation constants, but required a high proportion of co-solvent to determine the first constant ($\log K_1$) due to low solubility of SKI-606 at high pH. The first macroscopic constant, being UV active, was readily measured using the spectrophotometric technique. Measuring the constants in different proportions of methanol:water solvent revealed the presence of an acidic amino proton with an unusually low $\log K(<20)$. Only two of the four protonation sites yielded a change in the UV spectrum, however, the protonation state of all sites was readily determined using NMR titrimetric methodology. The use of NMR also allowed for the unambiguous assignment of each protonation site. It was also found that it was not possible to access the microscopic constants from the spectrophotometric data, but as the extent of protonation of all of the sites could be monitored using NMR the microscopic constants were calculated from a combination of the potentiometric and NMR data. Our experience in profiling the acid–base properties of SKI-606 strengthens our conviction that it is necessary to employ a combination of techniques when profiling the acid–base properties of complex drug molecules.

Acknowledgement

We thank J. E. A. Comer for reviewing the manuscript and for various helpful comments.

References

[1] P. Macheras, C. Reppas, J.B. Dressman, Biopharmaceutics of Orally Administered Drugs, Ellis Horwood, London, 1995.
[2] L.Z. Benet, J.E. Goyan, J. Pharm. Sci. 56 (1967) 665–680.
[3] Y.C. Martin, J. Med. Chem. 48 (2005) 3164–3170.
[4] A. Albert, E.P. Serjeant, The Determination of Ionisation Constants, Chapman and Hall, London, 1984.
[5] Z. Szakács, M. Kraszni, B. Noszál, Anal. Bioanal. Chem. 378 (2004) 1428–1448.
[6] J.A. Goldman, L. Meites, Anal. Chim. Acta 30 (1964) 28–33.
[7] K. Takács-Novák, K.J. Box, A. Avdeef, Int. J. Pharm. 151 (1997) 235–248.
[8] R.I. Allen, K.J. Box, J.E.A. Comer, C. Peake, K.Y. Tam, J. Pharm. Biomed. Anal. 17 (1998) 699–712.
[9] R.C. Mitchell, C.J. Salter, K.Y. Tam, J. Pharm. Biomed. Anal. 20 (1999) 289–295.
[10] D.H. Boschelli, Med. Chem. Rev.-Online 1 (2004) 457–463.
[11] J.M. Golas, K. Arndt, C. Etienne, J. Lucas, D. Nardin, J. Gibbons, P. Frost, F. Ye, D.H. Boschelli, F. Boschelli, Cancer Res. 63 (2003) 375–381.
[12] A. Avdeef, J.E.A. Comer, S.J. Thomson, Anal. Chem. 65 (1993) 42–49.
[13] K.Y. Tam, K. Takács-Novák, Anal. Chim. Acta. 434 (2001) 157–167.
[14] K.Y. Tam, L. Quéré, Anal. Sci. 17 (2001) 1203–1208.
[15] K. Mazák, A. Nemes, B. Noszál, Pharm. Res. 16 (1999) 1757–1763.

[16] Z. Szakács, S. Béni, Z. Varga, L. Örfi, G. Kéri, B. Noszál, J. Med. Chem. 48 (2005) 249–255.
[17] K. Takács-Novák, K.Y. Tam, J. Pharm. Biomed. Anal. 21 (2000) 1171–1182.
[18] B. Noszál, J. Phys. Chem. 90 (1986) 4104–4110.
[19] J.B. Dressman, G.L. Amidon, C. Reppas, V.P. Shah, Pharm. Res. 15 (1998) 11–22.
[20] R. Thaimattam, P.R. Daga, R. Banerjee, J. Iqbal, Bioorg. Med. Chem. 13 (2005) 4704–4712.